A woven 2D touchpad sensor and a 1D slide sensor using soft capacitor fibers

2012 Smart Mater. Struct. 21 015010

(http://iopscience.iop.org/0964-1726/21/1/015010)

IOP Publishing — Smart Materials and Structures
Smart Mater. Struct. **21** (2012) 015010 (10pp) doi:10.1088/0964-1726/21/1/015010

A woven 2D touchpad sensor and a 1D slide sensor using soft capacitor fibers

Stephan Gorgutsa, Jian Feng Gu and Maksim Skorobogatiy

Genie Physique, Ecole Polytechnique de Montreal, Montreal, H3C 3A7, Canada

E-mail: maksim.skorobogatiy@polymtl.ca

Received 17 August 2011, in final form 16 November 2011
Published 19 December 2011
Online at stacks.iop.org/SMS/21/015010

Abstract
Recently reported soft conductive-polymer-based capacitor fibers are used to build a fully woven 2D touchpad sensor and a 1D slide sensor. An individual capacitor fiber features a swiss-roll like structure having two dielectric and two conductive polymer films rolled together in a classic multilayer capacitor configuration. The soft fibers of sub-1 mm outer diameter are fabricated using a fiber drawing procedure from a macroscopic polymeric preform. An individual capacitor fiber is then demonstrated to act as a distributed sensor that allows the touch position to be determined by measuring the fiber's AC response. In other words, a single fiber acts as a 1D slide sensor. Furthermore, we develop an electrical ladder network model to predict the distributed sensor properties of an individual fiber and show that this model describes the experimental measurements very well. Finally, a two-dimensional touchpad sensor is presented. The sensor is built by weaving a one-dimensional array of capacitor fibers in parallel to each other. The performance of the touchpad sensor is then characterized.

(Some figures may appear in colour only in the online journal)

1. Introduction

Touch sensing as a human interface device (HID) technology is becoming increasingly popular and ubiquitous finding its applications in smart phones, computers and responsive garments to name a few. Various touch sensing systems have been developed based on different physical principles including resistive, capacitive, infrared, surface acoustic wave, electromagnetic, near field imaging, etc. Resistive [1] and capacitive [2] methods have been widely used in conventional touch screens of commercial products such as mobile phones, PDAs, and consumer electronics devices. Resistive touch screens are composed of two material sheets that are coated with a resistive material, commonly indium tin oxide (ITO), and separated by an air gap or microdots. When a finger presses the screen, the two sheets are connected at the touch position which changes the current flow in the screen. A sensing circuit then detects changes and locates the touch position. A capacitive touch sensor is based on the capacitive coupling effect. A typical design involves coating the screen with a thin, transparent metallic layer, in order to form a collection of capacitors on the surface. When a user touches the surface, the disturbance caused by the finger changes the capacitance and current that flows on the display.

A significant limitation for most of these technologies is that they are only capable of detecting a single touch. Multi-touch techniques allow touch screens to recognize touches of multiple fingers or inputs of multiple persons simultaneously. Multi-touch detection mechanisms can be classified into three categories: sensor array, capacitive sensing, and vision and optical based ones. A sensor array touch surface consists of a grid of touch sensors that work independently. When a user exerts multiple touches on the surface, the system can identify activated sensors and determine these touch positions simultaneously. An example is the FMTSID (fast multiple-touch-sensitive input device) [3], one of the first multi-point touch sensor-based devices. The system consists of a sensor matrix panel, the ranks of select register, an A/D converter and a control CPU. The design of the sensor matrix is based on the technique of capacitance measurement between a fingertip and a metal plate. A capacitive touch method uses the capacitive coupling between two conductors to sense a touch. Typically, the touch surface contains a mesh of horizontal and vertical

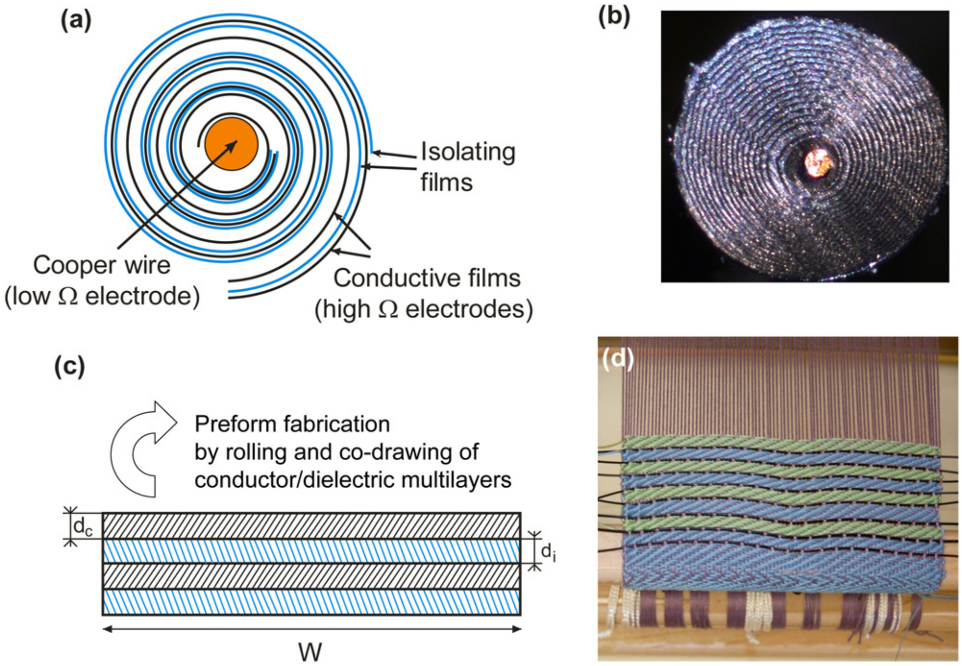

Figure 1. (a) Schematic of a capacitor fiber featuring a spiraling multilayer comprising two conductive and two isolating films. The black curves represent the two conductive films, while the blue curves represent the isolating films. (b) Photo of the cross section of a drawn capacitor fiber (900 μm in diameter) with a copper wire (100 μm in diameter) embedded in the center. A multilayer ($N \sim 30$) structure can be clearly seen. (c) The fiber preform is made by co-rolling four polymer layers (two conductive and two isolating) into a swiss-roll structure. The number of resultant layers in the spiral structure is proportional to the width of the unrolled multilayer. In the drawn fiber, the thicknesses of the conductive d_c and isolating d_i layers can be smaller than 10 μm, while the unwrapped width W of the layers fitting into a 1 mm diameter fiber can be in excess of 3 cm. (d) Weaving a two-dimensional touchpad sensor on a Dobby loom.

antennas which function as either transmitters or receivers of electric signals. Examples based on this technology include Rekimoto's SmartSkin [4], and DiamondTouch [5] developed by Dietz and Leigh.

In addition to touch screens, touch sensors with force sensing ability have been studied as tactile sensors for many years [6]. Such sensors have found their applications in artificial skin for robot applications [7], minimally invasive surgery [8], wearable computers [9], and mobile or desktop haptic devices [10]. To date tactile sensors have mainly focused on silicon-based sensors that use piezoresistive [11, 12] or capacitive sensing mechanisms [13–15]. Silicon tactile sensors have limitations of mechanical brittleness, and hence are not capable of sustaining large deformations. Polymer-based tactile sensing approaches that use piezoelectric polymer films [16–18], pressure-conductive rubber [19], carbon fiber based polymer composite [20] and conductive polymers [21], have been reported as well. These sensors provide good resolution but the applied force range is low due to the limited thickness of a membrane.

In this paper we demonstrate that the soft capacitor fibers recently developed in our laboratory [22] are well suited for integration into woven textile products, and that these electroactive fibers can be used as building blocks for textile-based slide sensors and touchpads. We start the paper with a description of the structure and fabrication technique of a capacitor fiber. We then continue with the study of the AC response of a single fiber and show that a single capacitor fiber can be used as a touch-based slide sensor. We, furthermore, introduce a theoretical model to describe the electrical response of a single capacitor fiber using an electrical ladder network model. Finally, we present the prototype of a woven touchpad sensor featuring a one-dimensional array of capacitor fibers, and then study the touchpad's performance.

2. Soft capacitor fibers as building blocks for textile touch sensors

Recently our group presented a novel, highly flexible fiber with high electric capacitance [22]. In its cross section the capacitor fiber features a swiss-roll structure where two conductive films (carbon-black-filled polyethylene (PE)) and two dielectric films (low density PE) are co-rolled to form a round multilayer capacitor (see figures 1(a) and (b)). The fiber is fabricated by drawing from a macroscopic preform. The fiber preform is made by periodically stacking four conductive and isolating layers (see figure 1(c)) and then rolling the multilayer into a swiss-roll configuration featuring a large central hole. The thus fabricated preform is a cylinder of a typical size of 30 cm in length and 2 cm in diameter. The all-polymer preform is then drawn at around 200 °C into a capacitor fiber. This fabrication technique is directly analogous to the one used in the manufacture of microstructured polymer optical fibers [23]. Additionally, a small-diameter (typically 50–150 μm) copper wire can be embedded into the fiber during the drawing process by passing it inside the fiber preform central hole

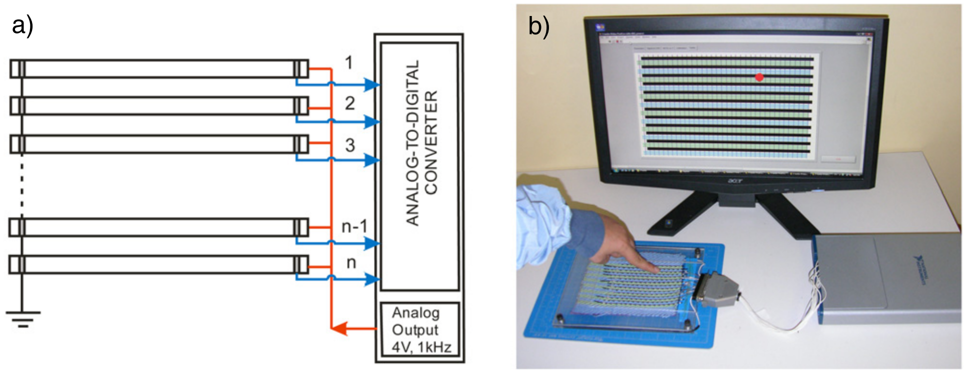

Figure 2. The woven touchpad sensor. (a) Schematic representation of the woven 2D touchpad sensor featuring a one-dimensional array of capacitor fibers. All the connections to and from the fibers are made using a 120 μm diameter copper wire (denoted by red lines). The fibers in the array have a common ground and a common source; however, they are interrogated individually. The analog output of the ADC board is used as a function generator that provides a sinusoidal signal at 1 kHz with an amplitude of 4 V. (b) Photograph of the woven touchpad connected to the ADC board, as well as the monitor image of a textile with an interpreted touch position.

and letting the preform collapse around the wire in the neckdown region. Introduction of a copper wire into the fiber drawing process actually improves the fiber drawability and eases connectorization of the resultant fibers in textile-based electrical circuits. In practical applications, the copper wire in the fiber center serves as a low resistivity electrode attached to one of the two high resistivity conductive plastic electrodes of a fiber capacitor. The other high resistivity conductive plastic electrode of a fiber is brought to the fiber surface to ease connectorization. Typical fibers fabricated using the above-mentioned fabrication procedure have a sub-millimeter diameter, contain at least 30 layers, and have a typical capacitance of 100 nF m^{-1}, which is almost three orders of magnitude higher than that of a standard coaxial cable of a comparable diameter.

At the same time, the soft, while highly elastic, mechanical nature of the fibers makes them easy to use in a conventional weaving process (figure 1(d)). In our laboratory we have used a table Dobby loom (Leclerc Voyager $15\frac{3}{4}''$ 4 s) to weave the fibers into a one-dimensional senor array integrated into a wool-based textile matrix (see figure 1(d)). The resulting 15 cm $\times$ 10 cm woven touchpad contained 15 capacitor fibers, each 12 cm long (see figure 2(b)).

The high resistivity of the conductive polymer electrodes together with their high capacitance endows the fiber with interesting electrical properties, which, as we will see in what follows, makes the fiber well suited for distributed sensing applications of touch. In a typical implementation of a touch sensor, we ground the outer fiber electrode (high Ω electrode) on one end, while applying the AC voltage to the copper wire (low Ω electrode) on the other end (see figure 2(a)). We then read out the voltage on the fiber outer electrode (high Ω electrode) at the same end where the copper wire is connectorized. In our experiments we find that the read out voltage is highly sensitive to the position of the touch along the fiber, which allows us to build a touchpad sensor that can localize in two dimensions the position of touch (figure 2(b)).

In our experimental setup the inner electrodes of all the fibers (copper wires) are connected to the analog voltage source integrated into the analog-to-digital converter (ADC)

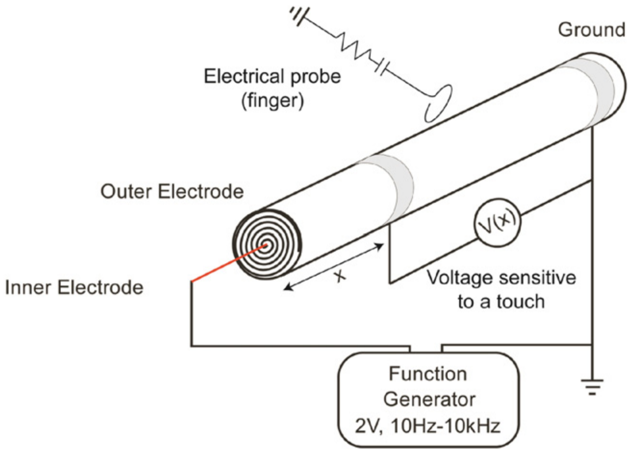

Figure 3. Schematic of a 1D slide sensor based on a single capacitor fiber.

card providing a sinusoidal signal at 1 kHz with an amplitude of 4 V. The outer electrodes of the fibers are connected to the individual channels of the ADC card (National Instruments USB-6343 X-series DAQ) in order to measure the voltage at their endpoints. The connections are made using thin copper wires (0.120 μm diameter) and secured with a conductive epoxy. The ADC board is plugged into a PC and the touch position can then be monitored on the computer screen via LabVIEW software.

2.1. Sensing of touch with a single fiber: a 1D slide sensor

In order to understand the sensing principle behind a touchpad we first consider the electrical response to touching of a single capacitor fiber. To characterize a single fiber we use the general electrical layout outlined earlier. In particular, a sinusoidal signal of voltage amplitude V_0 and constant frequency (10 Hz–10 kHz) is provided by an external function generator and is applied to the copper wire electrode of a fiber (see figure 3). The voltage response is acquired using a sliding contact on the outer electrode of the fiber (high Ω

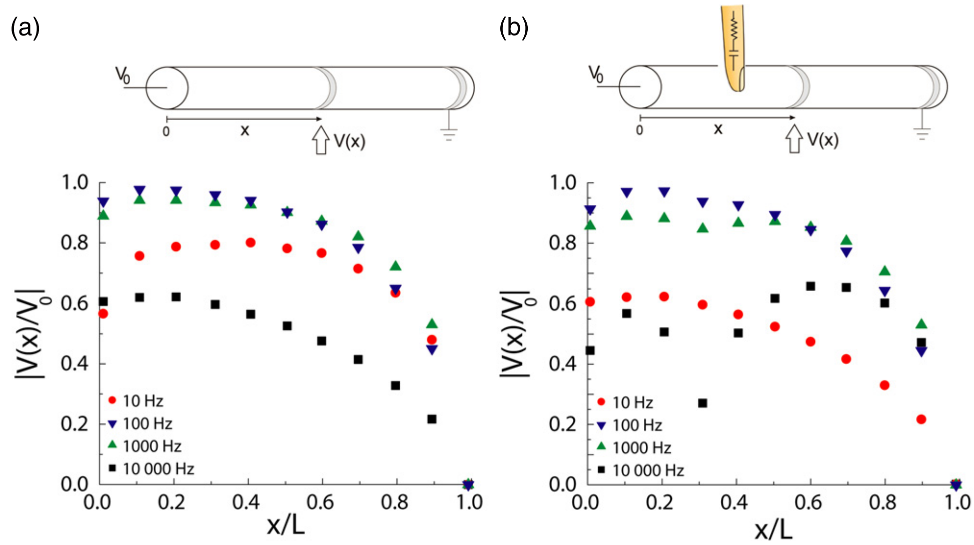

Figure 4. Voltage distribution along the outer fiber electrode for (a) an isolated fiber, (b) a fiber touched with an equivalent human probe. The four data sets correspond to the different driving frequencies of 10 Hz, 100 Hz, 1 kHz and 10 kHz. The voltage distribution along the fiber touched with a probe shows a dip in the vicinity of the touching position.

electrode). The sliding contact is connected to the oscilloscope (GDS-1022, Good Will Instrument Co., Ltd) through a 10× probe (GTP-060A-4, Good Will Instrument Co., Ltd). This arrangement allows measurement of the voltage distribution along the fiber length both when the fiber is touched and when it is not. As a human body is largely composed of conductive electrolytes covered with a layer of dielectric skin, the human body can be approximated by an equivalent electrical circuit comprising a resistor connected in series to a capacitor. Typical values of effective resistance and capacitance are 1.44 kΩ and 150 pF respectively. In our experimental studies of a single fiber's response to touching, we use an equivalent human probe with these effective electrical parameters to guarantee repeatability between measurements and to simplify the theoretical interpretation of the acquired data.

2.1.1. Experimental characterization of a single capacitor fiber and a 1D slide sensor. In figure 4 we present the voltage distribution along the fiber length for an isolated fiber (figure 4(a)), and for a fiber that is touched with an equivalent human probe (figure 4(b)). Here x/L represents the normalized position of the sliding contact along the fiber length. The fiber length used in our experiments was $L = 12.3$ cm. $|V(x)/V_0|$ represents the voltage measured by the sliding contact along the outer electrode of a capacitor fiber. When using the equivalent human probe (figure 4(b)), we fix it at the position $x/L = 0.3$. The different data sets in figure 4 correspond to the four different frequencies of the function generator used in our measurements (10 Hz, 100 Hz, 1 kHz, 10 kHz).

In the DC case (not shown in the figures), the voltage along the outer electrode of a capacitor is constant and zero as the capacitor fiber breaks the DC electrical circuit. For an isolated fiber (figure 4(a)) in the AC case, the voltage distribution along the fiber length shows the same trend at all frequencies. In particular, it saturates exponentially fast from zero at the grounded end to some maximal value at the other end of the fiber. The maximal voltage amplitude at the outer fiber electrode is strongly dependent on the operation frequency and it reaches its maximum at frequencies between 100 Hz and 1 kHz. When the fiber is touched with an equivalent human probe, the voltage distribution along the fiber's outer electrode shows high sensitivity to the operation frequency (figure 4(b)). Thus, at low driving frequencies (10, 100 Hz) the voltage distribution along the fiber's outer electrode is virtually unchanged by the touch. At higher frequencies (above 100 Hz) a dip appears in the voltage distribution in the vicinity of the point of contact with an equivalent human probe. Finally, at high frequencies (above 1 kHz) this dip becomes very pronounced and easy to detect. The overall frequency response of the capacitor fiber can be understood from basic electric circuit theory. Thus, the fiber used in these experiments had a capacitance per unit length of $C = 93$ nF m^{-1} and a transverse resistance of $R_t = 14.5$ kΩ m (bulk resistance of conductive layers 4.8 Ω m). The characteristic frequency associated with the corresponding RC circuit is $\nu = 1/(2\pi R_t C) = 120$ Hz. The electric response of a capacitor fiber is, in fact, that of a high pass filter. Namely, at frequencies well below 120 Hz the fiber operates in a quasi-DC regime where it simply breaks the electrical circuit. The fiber's response to touch is, therefore, minimal at low frequencies. At frequencies comparable to or higher than 120 Hz the capacitor fiber acts as a relatively low resistivity distributed complex impedance. At these higher frequencies touching the capacitor fiber can modify significantly the local current flows and voltage distributions, thus resulting in sensitivity of its various electrical parameters to touching.

From figure 4(b) it is clear that when operating at higher driving frequencies the touch position can be determined from the dip in the voltage distribution along the fiber's outer electrode. For practical implementation of a slide sensor it

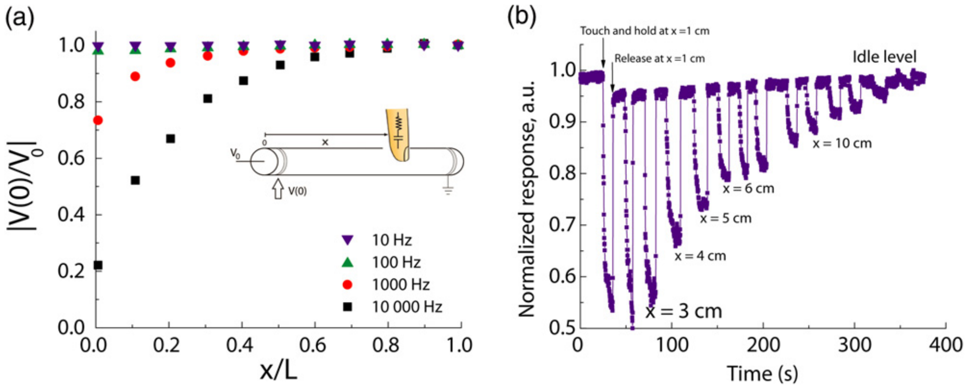

Figure 5. Detection of touch with a 1D slide sensor. (a) Voltage measured at the extremity of a capacitor fiber opposite to the fiber's grounded end. (b) Typical time resolved response of a slide sensor. The dips in the measured voltage correspond to the touch and release events.

is, however, inconvenient to require the knowledge of the voltage distribution across the whole fiber length. Therefore, the important question is whether the position of the touch can be determined by continuously measuring the voltage at a single fixed point on the fiber's outer electrode. To answer this question in figure 5(a) we present the value of voltage as measured at the fiber extremity ($x = 0$) as a function of the touch position along the fiber. As before, x/L represents the touch position of the equivalent human probe, while $|V(0)/V_0|$ represents the voltage measured at the fiber end opposite to the grounded end. We observe that for driving frequencies above 100 Hz, the voltage at the fiber extremity changes significantly depending on the position of the touch. In turn, this allows building of a 1D sliding sensor with a convenient acquisition procedure based on a single point measurement.

Finally, a 1D slide sensor was characterized in a realistic setting with a student touching the sensor consecutively at different positions along the fiber's length. This time the sensor was touched with an actual finger and not an equivalent probe. The driving frequency was 1 kHz and it was provided by the analog output of an ADC card. The same card was also employed as a signal acquisition unit with an acquisition rate of 20 kHz. Such high acquisition rates were only used for the purpose of resolving the time response of a sensor and in practice significantly slower acquisition rates (<10 Hz) could be used. To deduce the touch position we continuously measured the voltage at the endpoint of the fiber's outer electrode. Figure 5(b) presents an example of the measured voltage as a function of time. To operate the sensor we first record for several seconds the voltage level ('idle' level) without touching the fiber. We then touch the sensor at $x = 1$ cm from the fiber end. At the moment of touch the signal drops very rapidly (in a matter of 1 s) to almost its equilibrium value; this is followed by a much slower (~10 s) relaxation to the actual equilibrium value. We believe that the fast time scale corresponds to a pure electrical response of the fiber, while the slow time scale corresponds to small pressure induced changes in the fiber's electrical parameter due to fiber deformation under touch. As soon as the finger is removed, the signal returns back to the 'idle' level in a matter of 0.2 s. Next, by touching, holding, and releasing the fiber at various positions along its length we can record a complete calibration curve. Then, the position of a touch can be determined from the voltage level at the bottom of a dip corresponding to a touching event. This is, of course, the simplest implementation of a touch sensor. To avoid person-dependent calibration of the sensor one can, for example, perform two voltage measurements from opposing sides of a fiber (by simultaneously flipping the ground from one side to the other), then use analytical models to extract the effective electrical parameters of a human finger and find the touch position.

2.1.2. Ladder network model and user-specific calibration procedure. To model the electrical response of the capacitor fibers we use an RC ladder network which is an extension of the method originally developed in [22].

First, we consider a stand-alone capacitor fiber without touching. We define the conductive polymer electrode transverse resistance as $R_t \approx r_t/L$, where the electrode resistivity is $r_t = \rho_v W/d_c$. We also use the following definitions: ρ_v is the volume resistivity of the conductive films, L is the length of the fiber, W and d_c denote respectively the width and thickness of the conductive electrodes wrapped in the fiber cross section (see figure 1(c)). To measure the transverse resistance one has to ensure that there are no longitudinal (along the fiber length) currents in the fiber. In practice, to deduce the transverse resistivity one covers the outer fiber electrode (high resistivity electrode) with a metallic foil, and then measures the fiber's AC response by applying the voltage between the inner copper electrode and the outer metallic foil.

Similarly, we define the conductive polymer electrode longitudinal resistance as $R_l \approx r_l L$, where the electrode's longitudinal resistivity is $r_l = \rho_v/(W d_c)$. To measure the longitudinal resistance one has to ensure that there are no transverse (perpendicular to the fiber length) currents in the fiber. In practice, it is difficult to measure the longitudinal resistivity directly. In principle, if the electrode length (fiber length) is much longer than the net width of a conductive electrode wrapped in the fiber cross section, the longitudinal resistivity can be deduced from the AC measurement where

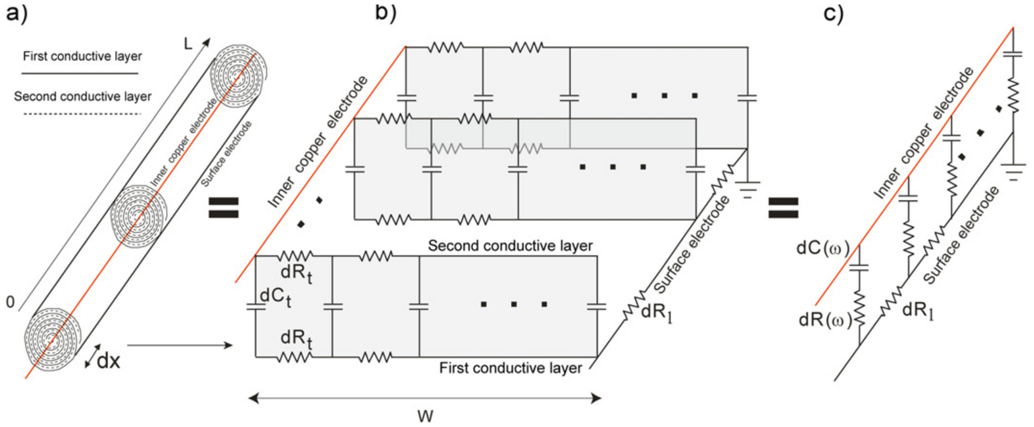

Figure 6. The ladder RC network model of a stand-alone capacitor fiber. (a) The fiber is modeled as a sequence of fiber dR_l (high resistivity outer cross sections of small length dx connected in series via longitudinal resistive electrode elements), while we assume that the inner copper electrode has a constant potential along its length. (b) The electrical response of an individual fiber cross section is modeled as an RC network where the transverse resistivity elements dR_t are connected via capacitance dC_t elements. (c) One can show that the equivalent circuit that describes the electrical response of an individual fiber cross section is given simply by the frequency dependent resistivity d$R(\omega)$ connected in series with the frequency dependent capacitance d$C(\omega)$. Finally, the electrical response of a fiber is modeled as another RC network with frequency dependent resistivity and capacitance.

the high resistivity outer electrode of a fiber is grounded on one end, while the inner high resistivity electrode of the fiber is connected to a voltage supply at the other end. Note that the low resistivity copper electrode has to be removed from the fiber for this measurement.

Finally, the total fiber capacitance is proportional to the fiber length, while the fiber capacitance per unit length is simply $C_t \approx 2\varepsilon_0 \varepsilon W/d_i$, where d_i is the thickness of the isolating films in the fiber, ε is the dielectric constant of the isolating films, and ε_0 is the permeability of vacuum. We note that the relatively high capacitance of our fibers is due to the small thickness of the isolating films, and the large net width of the conductive layers. Thus, a typical fiber features conductive and isolating layers with thicknesses smaller than 10 μm, while the net width W of the layers wrapped into a 1 mm diameter fiber can be in excess of 3 cm.

To model the electrical response of a fiber we consider it as a sequence of thin cross sections of length dx (figure 6(a)) each having a longitudinal resistance d$R_l = r_l\,$dx. We then consider the electrical response of an individual cross section, while assuming that along the fiber length the individual fiber sections are connected via longitudinal resistance elements dR_l (figure 6(b)). The electrical response of an individual fiber cross section is modeled as an RC network where transverse resistivity elements d$R_t = r_t/$dx are connected via capacitance d$C_t = C_t\,$dx elements. In [22] we show that the equivalent circuit that describes the electrical response of an individual fiber cross section of length dx is given by the frequency dependent resistivity d$R(\omega)$ connected in series with the frequency dependent capacitance d$C(\omega)$, where

$$\mathrm{d}C(\omega) = -\frac{\mathrm{d}x}{\omega r_t \,\mathrm{Im}(f(B))}, \tag{1}$$

$$\mathrm{d}R(\omega) = \left(\frac{1}{2} + \mathrm{Re}(f(B))\right)\frac{r_t}{\mathrm{d}x}, \tag{2}$$

and $f(B) = \frac{1+\cosh(B)}{B\sinh(B)}$; $B = \sqrt{2\mathrm{j}\omega r_t C_t}$.

The electrical response of a stand-alone fiber can, therefore, be modeled as another RC ladder with frequency dependent parameters d$R(\omega)$, d$C(\omega)$, and frequency independent parameters dR_l (see figure 6(c)).

Now that the model for a stand-alone capacitor fiber is defined, we modify it slightly in order to analyze a 1D slide sensor. In particular, the fiber is assumed to be touched at a position x_b with a finger having effective electric parameters $R_b = 1.44$ kΩ, $C_b = 150$ pF. Moreover, to simplify comparison with experiment we include in our model the effective circuit of an oscilloscope probe used in our measurements. The probe is attached at a position x_p on the fiber surface (see figure 7), and the effective circuit parameters of the probe and oscilloscope are $R_p = 10$ MΩ, $C_p = 200$ pF. The necessity to include the effective circuit of a probe into the model comes from the realization that the resistance of the standard 10$\times$ probe (10 MΩ) used in our experiments has the same order of magnitude as the transverse resistance of the short fiber segments used in our studies. For example, the transverse resistance of the 10 cm-long fiber pieces typically ranges from 0.1 to 1 MΩ. Moreover, one can show that at frequencies lower than $\nu \approx 1/(2\pi R_p C_b) \approx 100$ Hz or higher than $\nu \approx 1/(2\pi R_b C_p) \approx 55$ kHz, the effective impedance of a probe becomes smaller than that of a finger; therefore the probe's effective circuit has to be included into the model to accurately explain the experimental measurements.

In figure 7 we distinguish three parts of an RC latter network. The first part is located to the left of the probe, where $i''(x)$ denotes the longitudinal current flowing in the polymer conductive film, while d$i''(x)$ denotes the transverse current flowing in the thin section of length dx. To the right of the probe, while still before the finger touch position the longitudinal and transverse currents in the polymer electrode are denoted as $i(x)$ and d$i(x)$. Finally, to the right of the touch position the corresponding currents are $i'(x)$ and d$i'(x)$. V_0 is the voltage difference between the inner copper electrode and

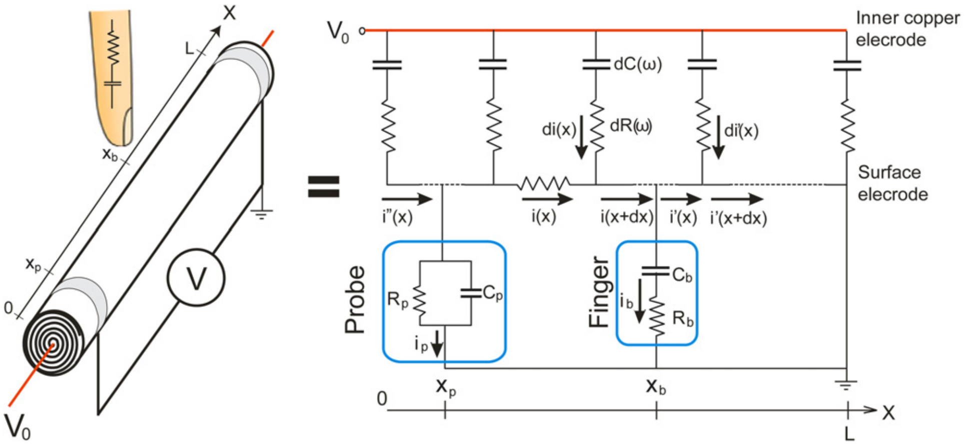

Figure 7. The ladder network model of a 1D slide sensor. The fiber is assumed to be touched at a position x_b with a finger having effective electric parameters R_b, C_b. Moreover, to simplify the comparison with experiment we include in our model the effective circuit (with parameters R_p, C_p) of an oscilloscope probe used in our measurements; the probe is attached at a position x_p.

the outer electrode at $x = L$. We also assume that the fiber material parameters are position and frequency independent. Furthermore, we consider that the probe is attached to the left of the touch position, $x_p < x_b$. We now apply Kirchhoff's voltage law and the current conservation law to the ladder circuit to arrive at the following equations for any position x along the fiber. Thus, using Kirchhoff's voltage law we get

$$\begin{aligned}
&0 < x < x_p; \\
&\quad \mathrm{d}i''(x)\left(\frac{1}{\mathrm{j}\omega\,\mathrm{d}C(\omega)} + \mathrm{d}R(\omega)\right) + \int_x^{x_p} r_l i''(l)\,\mathrm{d}l = V_0 - V(x_p) \\
&x = x_p; \qquad i_p \frac{R_p}{1+\mathrm{j}\omega C_p R_p} = V(x_p) \\
&x_p < x < x_b; \\
&\quad \mathrm{d}i(x)\left(\frac{1}{\mathrm{j}\omega\,\mathrm{d}C(\omega)} + \mathrm{d}R(\omega)\right) + \int_x^{x_b} r_l i(l)\,\mathrm{d}l = V_0 - V(x_b) \\
&x = x_b; \qquad i_b\left(\frac{1}{\mathrm{j}\omega C_b} + R_b\right) = V(x_b) \\
&x_b < x < L; \\
&\quad \mathrm{d}i'(x)\left(\frac{1}{\mathrm{j}\omega\,\mathrm{d}C(\omega)} + \mathrm{d}R(\omega)\right) + \int_x^{L} r_l i'(l)\,\mathrm{d}l = V_0.
\end{aligned} \tag{3}$$

Using the current conservation law we get

$$\begin{aligned}
&0 < x < x_p; && i''(x) + \mathrm{d}i''(x) = i''(x+\mathrm{d}x) \\
&x = x_p; && i''(x_p) = \mathrm{i}(x_p) + i_p \\
&x_p < x < x_b; && i(x) + \mathrm{d}i(x) = i(x+\mathrm{d}x) \\
&x = x_b; && i(x_b) = i'(x_b) + i_b \\
&x_p < x < L; && i'(x) + \mathrm{d}i'(x) = i'(x+\mathrm{d}x).
\end{aligned} \tag{4}$$

Finally, the boundary conditions are

$$i''(0) = 0. \tag{5}$$

To solve these equations, we can first differentiate equations (3) with respect to x to obtain three similar second order differential equations with respect to i, i' or i'' of the following form:

$$\frac{\mathrm{d}^2 i(x)}{\mathrm{d}x^2}\left(\frac{1}{\mathrm{j}\omega\,\mathrm{d}C(\omega)/\mathrm{d}x} + \mathrm{d}x\,\mathrm{d}R(\omega)\right) - r_l i(x) = 0. \tag{6}$$

Then, in each of the three sections of the fiber, we can write solution for the currents as

$$i = C_1 \mathrm{e}^{\tilde{B}x} + C_2 \mathrm{e}^{-\tilde{B}x}, \qquad i' = C_3 \mathrm{e}^{\tilde{B}x} + C_4 \mathrm{e}^{-\tilde{B}x}, \qquad i'' = C_5 \mathrm{e}^{\tilde{B}x} + C_6 \mathrm{e}^{-\tilde{B}x}, \tag{7}$$

where

$$\tilde{B} = \sqrt{\frac{r_l}{\left(\frac{1}{\mathrm{j}\omega\,\mathrm{d}C(\omega)/\mathrm{d}x} + \mathrm{d}x\mathrm{d}R(\omega)\right)}} = \sqrt{\frac{r_l}{r_t\left(\frac{1}{2} + f(B)\right)}}, \tag{8}$$

and B, $f(B)$ are defined in (1) and (2). Insertion of expressions (7) into the remaining equations (3)–(5) results in a set of linear equations from which the constants $C_1 - C_6$ can be determined. Finally, from the known current distributions the voltage distribution in each section can be easily found as

$$V(x) = V_0 - \frac{\mathrm{d}^2 i(x)}{\mathrm{d}x^2}\left(\frac{1}{\mathrm{j}\omega\,\mathrm{d}C(\omega)/\mathrm{d}x} + \mathrm{d}x\,\mathrm{d}R(\omega)\right). \tag{9}$$

2.1.3. Comparison of the experimental data with the predictions of a theoretical model. In figure 8 we present the experimental data and theoretical RC ladder model (3)–(9) predictions for the dependence of voltage measured at $x_p = 0$ as a function of the equivalent human probe touch position x_b. In each graph, different sets of curves correspond to distinct fibers which are different from each other in a single parameter. Thus, in figure 8(a) we present measurements of three fibers which were drawn using preforms containing different numbers of conductive layers, and, as a consequence, have different capacitances. The preforms were drawn using the same temperature profile and drawing speed so as to guarantee similar values of the bulk resistivities of the polymer electrodes. Then, the fiber geometrical parameters such as layer thicknesses,

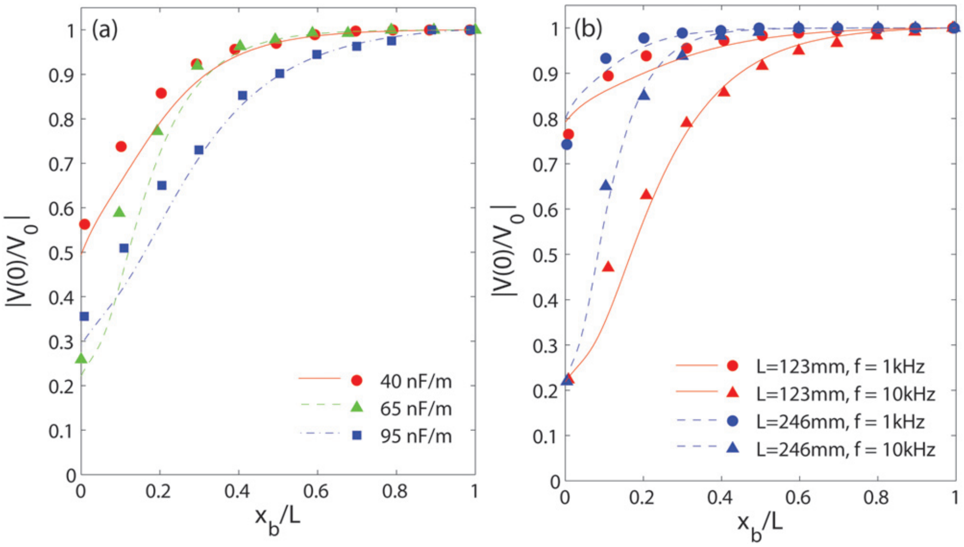

Figure 8. Fiber response to the touch of the equivalent human probe—comparison between predictions of the RC ladder model and experimental data. (a) Response at 10 kHz of three distinct fibers of the same length and different capacitances $C_t = 40, 65, 95$ nF m^{-1}. The rest of the geometrical and electrical parameters of the fibers are similar to each other. (b) Response at 1 kHz and 10 kHz of two distinct fibers of the different lengths. The rest of the geometrical and electrical parameters of the fibers are identical to each other as the shorter fiber was obtained by cutting a longer fiber in half.

electrode width and fiber length were measured using the optical microscope. The parameters of the oscilloscope effective circuit were measured independently. Finally, the bulk resistivity of the conductive layers in a fiber was measured as in [22] by wrapping the fiber's outer electrode into a foil and then extracting the transverse resistivity and, consequently, the bulk resistivity of the conductive layers from the fiber's AC response. In this arrangement the currents are purely transverse and the RC ladder model was shown [22] to give precise fits for the bulk resistivity parameter. We then use all these model parameters found in the independent measurements to predict the response of the fiber to the touch. From figure 8(a) we see that at the operating frequency of 10 kHz the experimental curves are very well described by the RC ladder model which does not use any fitting parameter.

Similarly, in figure 8(b) we present the fiber response to touch for two identical fibers of different lengths. In these experiments we first use a fiber of 24.6 cm in length and then cut it in half to 12.3 cm and repeat the measurement. The rest of the input parameters necessary for the use of a theoretical model were measured as described above. From the figure we see that the fiber response is very well described by the RC ladder model both at 1 and 10 kHz operating frequencies. Moreover, we see that this particular fiber becomes insensitive to touch if the touch point x_b is further than 10 cm from the measuring point x_p.

The measurement of fiber response as a function of fiber length presented in figure 8(b) brings about an important question about the maximal length of a 1D slide sensor, and about the optimal frequency of operation. We note that the functional form of the currents (7) flowing between the probe and the measurement point is exponential with the characteristic length

$$\tilde{L} = \frac{1}{\mathrm{Re}(\tilde{B})} = \frac{W}{\sqrt{2}} \frac{1}{\mathrm{Re}((1+2f(B))^{-\frac{1}{2}})}, \tag{10}$$

where we used $\sqrt{r_t/r_l} = W$. We now use asymptotic expansions of the function $f(B)$:

$$f(B) = \frac{1+\cosh(B)}{B\sinh(B)} \underset{B=\sqrt{2j\omega r_t C_t}}{=} \begin{cases} \dfrac{1}{B}, & \omega \gg \dfrac{1}{r_t C_t}, \\ \dfrac{2}{B^2}, & \omega \ll \dfrac{1}{r_t C_t}, \end{cases} \tag{11}$$

to get the following limiting values for the characteristic length of the current decay:

$$\tilde{L} = \frac{W}{\sqrt{2}} \begin{cases} 1, & \omega \gg \dfrac{1}{r_t C_t}, \\ \dfrac{1}{\sqrt{\omega r_t C_t}}, & \omega \ll \dfrac{1}{r_t C_t}. \end{cases} \tag{12}$$

Note that for the slide sensor of length L to be sensitive along its whole length we have to require that $L \sim \tilde{L}$. From expressions (12) this means that at high frequencies $\omega \gg 1/(r_t C_t)$ the maximal sensor length is limited by the net width of the polymer electrode wrapped into the fiber cross section. Note that for most of our fibers the region of high frequency is in the vicinity of or above 1 kHz. Furthermore, in a typical fiber of $D = 1$ mm diameter, we can currently fit $N \sim 10$–50 turns of the conductive electrode, which results in a net width of a conductive electrode in the fiber of $W \sim \pi DN \sim 3$–15 cm. Therefore, for operation frequencies in the vicinity of or above 1 kHz, the maximal length of the capacitor fiber-based slide sensor is currently limited to several tens of centimeters.

In principle, operation at lower frequencies allows matching of the fiber length and the characteristic current decay length $L \sim \tilde{L}$ for any desired length of fiber. This,

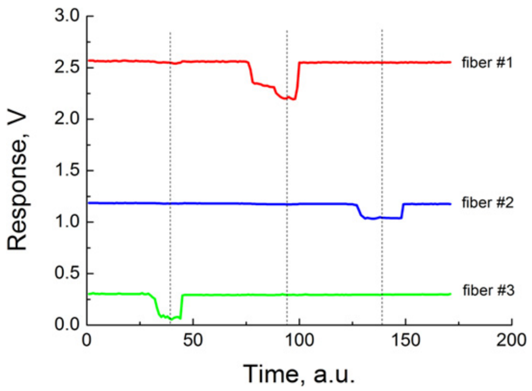

Figure 9. Recorded voltage response as a function of time for three neighboring fibers in the woven touchpad. No detectable cross-talk between the fibers was observed. The dips on the graphs correspond to the individual touch events that take place at different moments in time.

however, demands very low operation frequencies, $\omega \sim (W/L)^2/(r_t C_t)$, that even for a relatively short 1 m-long fiber can be as low as 1–10 Hz. Operation at low frequencies, however, is prone to strong electrical interference and noise. Moreover, at low frequencies ~1 Hz the finger has a very large impedance ≫1 MΩ, which is mismatched with that of our fiber. This makes the sensor of very low sensitivity at low frequencies.

2.2. Crosstalk between fibers in a 1D fiber array (2D touchpad sensor)

Finally, we address the question of crosstalk between the fibers in the woven 2D touchpad sensor. As discussed earlier, the sensor comprises a 1D fiber array separated by 1 cm of textile and is presented in figures 1 and 2. In principle, false responses in our system could be induced by cross-talk between individual fibers that may lead to interference effects between measured signals. In this case the electrical signal at one channel may induce a signal at another channel which might be detected as a false touch. In figure 9 we show an example of a typical recorded voltage response as a function of time for three neighboring fibers in the touchpad. No detectable cross-talk between the fibers was observed during recording. The dips on the graphs correspond to the individual touch events that take place at different moments in time. As can be seen in figure 9, after each touch and release, all the sensor channels successfully return back to the idle state. Despite the fact that in the simplest interrogation configuration each individual fiber incorporated into the textile is not multi-touch sensitive (only the touch closest to the outer electrode will be detected), the absence of inter-channel cross-talk enables simultaneous interrogation of the individual slide sensors. In this sense a 2D touchpad has a partial multi-touch functionality.

3. Conclusion

In conclusion, we have demonstrated that conductive-polymer-based capacitor fibers can be used to build a fully woven 2D touchpad sensor and a 1D slide sensor. An individual capacitor fiber was demonstrated to act as a distributed sensor that allows determination of the touch position along its length by measuring the fiber's AC response. In other words, a single fiber acts as a 1D slide sensor. A theoretical RC ladder model was developed and shown to describe successfully the experimental sensor performance. Then, a fully woven two-dimensional touchpad sensor was presented. The sensor was built by weaving a one-dimensional array of capacitor fibers in parallel to each other. The performance of the touchpad sensor was then characterized and the absence of inter-channel crosstalk was confirmed. It was concluded that the 2D touchpad has partial multi-touch functionality.

References

[1] Cok R S, Bourdelais R R and Kaminsky C J 2004 Flexible resistive touch screen *US Patent Specification* 0212599 A1
[2] Kalendra P W and Piazza W J 1994 Automatic calibration of a capacitive touch screen used with a fixed element flat screen display panel *US Patent Specification* 5283559
[3] Lee S, Buxton W and Smith K C 1985 A multi-touch three-dimensional touch-sensitive tablet *Proc. SIGCHI Conf. on Human Factors in Computing Systems* pp 21–5
[4] Rekimoto J 2002 SmartSkin: an infrastructure for freehand manipulation on interactive surfaces *Proc. SIGCHI Conf. on Human Factors in Computing Systems* pp 113–20
[5] Dietz P and Leigh D 2001 DiamondTouch: a multiuser touch technology *Proc. UIST, 14th Annu. ACM Symp. on User Interface Software and Technology* pp 219–26
[6] Dahiya R S, Metta G, Valle M and Sandini G 2010 Tactile sensing—from humans to humanoids *IEEE Trans. Robot.* **26** 1–20
[7] Engel J, Chen J and Liu C 2003 Development of polyimide flexible tactile sensor skin *J. Micromech. Microeng.* **13** 359–66
[8] Eltaib M E H and Hewit J R 2003 Tactile sensing technology for minimal access surgery—a review *Mechatronics* **13** 1163–77
[9] Hoshi T and Shinoda H 2006 A sensitive skin based on touch-area-evaluating tactile elements *Proc. Symp. on Haptic Interfaces for Virtual Environment and Teleoperator Systems* pp 89–94
[10] Ruspini D C, Kolarov K and Khatib O 1997 The haptic display of complex graphical environments *Proc. 24th Annu. Conf. on Computer Graphics and Interactive Techniques* pp 345–52
[11] Beebe D J, Hsieh A S, Denton D D and Radwin R G 1995 A silicon force sensor for robotics and medicine *Sensors Actuators* A **50** 55–65
[12] Wolffenbuttel M R and Regtien P P L 1991 Polysilicon bridges for the realization of tactile sensors *Sensors Actuators* A **26** 257–64
[13] Chu Z, Sarro P M and Middelhoek S 1995 *Transducers* **1** 656
[14] Gray B L and Fearing R S 1996 *Proc. IEEE Int. Conf. on Robotics and Automation* p 1
[15] Leineweber M, Pelz G, Schmidt M, Kappert H and Zimmer G 2000 *Sensors Actuators* A **84** 236
[16] Dario P and de Rossi D 1985 Tactile sensors and gripping challenge *IEEE Spectr.* **22** 46–52
[17] Kolesar E S, Dyson C S, Reston R R, Fitch R C, Ford D G and Nelms S D 1996 Tactile integrated circuit sensor realized

with a piezoelectric polymer *Proc. 8th IEEE Int. Conf. Innovative Syst. Silicon* pp 372–81

[18] Yuji J and Sonoda C 2006 A PVDF tactile sensor for static contact force and contact temperature *Proc. IEEE Sens.* pp 738–41

[19] Shimojo M, Namiki A, Ishikawa M and Makino R 2004 A tactile sensor sheet using pressure conductive rubber with electrical-wires stitched method *IEEE Sensors. J.* **4** 589–95

[20] Park C-S, Park J and Lee D-W 2009 A piezoresistive tactile sensor based on carbon fibers and polymer substrates *Microelectron. Eng.* **86** 1250–3

[21] Kim K, Lee K R, Kim W H, Park K-B, Kim T-H, Kim J-S and Pak J J 2009 Polymer-based flexible tactile sensor up to 32×32 arrays integrated with interconnection terminals *Sensors Actuators* A **156** 284–91

[22] Gu J F, Gorgutsa S and Skorobogatiy M 2010 Soft capacitor fibers using conductive polymers for electronic textiles *Smart Mater. Struct.* **19** 115006

[23] Gao Y, Guo N, Gauvreau B, Rajabian M, Skorobogata O, Pone E, Zabeida O, Martinu L, Dubois C and Skorobogatiy M 2006 Consecutive solvent evaporation and co-rolling techniques for polymer multilayer hollow fiber preform fabrication *J. Mater. Res.* **21** 2246–54